

Mechanical and Energy Engineering

**Crack Growth Behavior through Wall Pipes under Impact Loading
And Moist Environment**

Ali Jamal Khaled
M Sc Student
Email: engalijamal93@gmail.com

Dr.Ahmed Abdul Hussain*
Assist. Professor
Email: ahmedrobot65@yahoo.com

ABSTRACT

This search concerns study the crack growth in the wall of pipes made of low carbon steel under the impact load and using the effect of moisture (rate of moisture 50%). The environmental conditions were controlled using high accuracy digital control with sensors. The pipe has a crack already. The test was performed and on two type of specimens, one has a length of 100cm and other have length 50cm. The results were, when the humidity was applied to the pipe, the crack would enhance to grow (i.e. the number of cycles needed to grow the crack will reduce). In addition, when the test performed on the specimens of length 50cm the number of cycles needed to grow the crack is increased due to the effect of bending stress on the pipes.

Key Words: cracks, crack initiation, crack growth.

نمو الصدوع وتصرفها خلال جدران الانابيب المعرضة لأحمال صدمية ومحيط رطب

الخلاصة

يتناول هذا البحث دراسة نمو الصدع في جدار الانابيب المصنوعة من الفولاذ منخفض الكربون تحت تأثير حمل الصدمة واستخدام تأثير الرطوبة بنسبة 50%. تم التحكم في الظروف البيئية باستخدام جهاز تحكم عالي الدقة مع أجهزة الاستشعار. الانابيب تحتوي على صدع مسبقا. الاختبار اجري على نوعين من النماذج أحد هذه الأنواع ذو طول 100سم والأخر ذو طول 50سم. عند اجراء الاختبار فإن النتائج كانت، عند تطبيق الرطوبة فإن عدد الدورات اللازمة لنمو الصدع سوف تقل. بالإضافة الى ذلك فإنه عند اجراء الاختبار على النماذج ذات الطول 50سم فإن عدد الدورات اللازم لنمو الشق سوف يزداد نتيجة لتأثير اجهاد الانحناء على الانابيب. **الكلمات الرئيسية:** الصدوع، نشوء الصدوع، نمو الصدوع

1. INTRODUCTION.

Bertram, 1999, defined the cracks as a discontinuity or break, which occur in solid (rigid) body, and it branded by having an initiation point (start point), and by growing from this point to finite size with time. Either leading or not to the separation of the original body in two or more parts. Crack growth depended on the loading conditions also on the environmental conditions. Loading conditions presents the type of load such as a static load, dynamic load, controlled load, controlled, grip. Environmental conditions like, temperature and corrosive atmosphere influence crack growth.

*Corresponding author

Peer review under the responsibility of University of Baghdad.

<https://doi.org/10.31026/j.eng.2019.01.01>

2520-3339 © 2019 University of Baghdad. Production and hosting by Journal of Engineering.

This is an open access article under the CC BY-NC license <http://creativecommons.org/licenses/by-nc/4.0/>.

Article received: 13/12/2017

Article accepted: 19/2/2018



Stein, 2004, there are three types of cracks in pipes happen due to several causes associated with their types, whereby the form of a crack, its dimension, and its course gives conclusions on its cause. Thus, it is possible that, on the one side, one cause results in several cracks at different places and, in the other side, one crack can have several causes. The three types are:

- 1- Longitudinal cracks
- 2- Lateral cracks
- 3- Cracks origination at a point

2. THE BEHAVIOR OF CRACKS

The behavior of fatigue cracks differs from that of long cracks because of the larger sensitivity to the microstructure. A greater size of the plastic zone is relative to the crack length, and a lesser level of crack finish. Advances have been made in the understanding of the fatigue crack growth process of cracks, and this understanding has been employed in the advance of analytical treatments of short fatigue crack growth. The study of fatigue crack growth behavior of cracks is one of the more active areas of research in the field of fatigue. Such cracks are of interest not only because their growth can inhabit an important portion of the fatigue lifetime but also because they can grow at an amount much higher or lower than might be expected on the basis on long crack behavior. Below are four kinds of cracks fatigue **Mcevely, 1979**:

- 1- Mechanical cracks (the crack length is less than plastic zone size)
- 2- Microstructural (the crack length is less than a critical microstructural)
- 3- Physical (the crack length is less than at which crack closure if fully developed usually less than 1 mm in length)
- 4- Chemical (the crack length may be up to 10 mm)

3. GOVERNNING DIFFERENTIAL EQUATION

Paris proposed the following equation for the correct crack propagation law

$$\frac{da}{dN} = C(\Delta k)^m \tag{1}$$

Where C and m are constant and they depended on the material that be used

This equation seemed to have a good correlation with the test data. However, if comparisons are made with the large range of data, such as a higher load ratio and crack growth rates, the correlations are not good. In fact, Equation (1) does not seem to be complete. Two effects occur which are not taken into account. One of this variation in the crack growth rate owing to the load ratio, R . the other is the instability of the crack growth when the value of the maximum stress intensity factor approaches to the fracture toughness of the material, K_c , **Forman, et al., 1967**.



4. CRITERIA OF CRACK GROWTH

Theoretical and experimental work contains different criteria and approaches for the study of the crack growth direction. Many of this study are based on the stress analysis of the crack tip zone. Erdogan and Sih first examined the angled crack. They suggested the MTS criteria based on the stress field existing just before the onset of fracture for prediction of the direction of the initial crack extension. According to the MTS criteria, the crack extends in the radial direction agreeing to the maximum tangential stress and the crack extension occur then this maximum reaches a critical value. Erdogan and Sih’s study was based on the presentation of the crack tip stress field in terms of stress function derived by Williams **Wasiluk and Golos, 2000**.

$$\phi = r^{3/2} f_1(\theta) + r^2 f_2(\theta) + r^{5/2} f_3(\theta) \tag{2}$$

For the first term, the stress is represented by:

$$\sigma_\theta = \frac{1}{\sqrt{2\pi r}} \cos \frac{\theta}{2} (k_1 \cos^2 \frac{\theta}{2} - k_2 \sin \theta) \tag{3}$$

$$\tau_{r\theta} = \frac{1}{2\sqrt{2\pi r}} \cos \frac{\theta}{2} [k_1 \sin \theta + k_2 (3 \cos \theta - 1)] \tag{4}$$

Erdogan and Sih suggested that the direction of crack growth is given by the condition:

$$\frac{dk_\theta}{d\theta} = 0 \tag{5}$$

Where:

$$k_\theta = \cos^2 \frac{\theta}{2} (k_1 \cos \frac{\theta}{2} - 3k_2 \sin \frac{\theta}{2}) \tag{6}$$

$$\cos \frac{\theta}{2} [k_1 \sin \theta + k_2 (3 \cos \theta - 1)] = 0 \tag{7}$$

A better covenant between the theoretical and experimental has been obtained by a representation of the stress field using the first two terms of the Eigenfunction expansion, Equation (2). In addition, by using a small but finite radius to locate the maximum value of σ_θ and this was shown by Williams and Ewing. The elastic strain energy dW stored in the parallel pipe of volume dV in the dominate Sih expresses zone of the strained plate:

$$\frac{dW}{dV} = \frac{1+\nu}{4E} [k_{1,2}(\sigma_x + \sigma_y)^2 + (\sigma_x - \sigma_y)^2 + 4(\tau_{xy})^2] \tag{8}$$

$$k_1 = \frac{1-\nu}{1+\nu} \quad \text{For plane stress} \tag{9}$$

$$k_2 = 1 - 2\nu \quad \text{For plane strain} \tag{10}$$



Papadopoulos used the elastic strain energy approach to propose a criterion of fracture, which takes into account the third stress invariant Det. (σ_{ij})

$$\text{Det.}(\sigma_{ij}) = \begin{vmatrix} \sigma_x & \sigma_{xy} \\ \sigma_{xy} & \sigma_y \end{vmatrix} \quad (11)$$

According to the Det. – criteria the angle of crack extension for the mixed mode loading is determined from the condition that the determinate of the stress tensor must take a maximum value. In a polar coordinate system, the relations express these conditions mathematically:

$$\frac{\partial \text{Det.}(\sigma_{ij})}{\partial \theta} \Big|_{\theta=\theta^*} = 0, \quad \frac{\partial^2 \text{Det.}(\sigma_{ij})}{\partial \theta^2} \Big|_{\theta=\theta^*} < 0 \quad (12)$$

The critical stress for crack initiation is calculated by:

$$\text{Det.}(\sigma_{ij}) = \text{Det.}(\sigma_{ij})_{cr} \quad (13)$$

5. CYCLIC LOAD EQUATIONS

The equations below are available for transverse crack ($\alpha = 90^\circ$) with and without internal pulse pressure, **Al Laham and Ainsworth, 1999**

$$p = w \left[1 + \sqrt{\frac{1+2hEA}{wt}} \right] \quad (\text{for impact load}) \quad (14)$$

$$I = \frac{\pi}{64} (OD^4 - ID^4) \quad (15)$$

$$\delta = \frac{l^3 p}{48EI} \quad (\text{For simply supported beam}) \quad (16)$$

$$\sigma = \frac{MY}{I} \quad (\text{Bending stress}) \quad (17)$$

$$\sigma_{\min} = -\sigma_{\max} \quad (18)$$

$$\beta = \frac{a_j}{r} \quad (19)$$

$$\rho_0 = \frac{a_j}{\sqrt{rt}} \quad (20)$$

$$G_2(\rho_0) = 1 + 0.19\rho_0 + 0.01\rho_0^2 \quad (21)$$

$$C_1 = 1 + \frac{0.7071(1-\beta \cot(\beta))}{\left(\frac{\cot(\pi-\beta)}{\sqrt{2}} + \sqrt{2} \cot(\beta)\right) \beta} \quad (22)$$

$$C_2 = 1 + \frac{0.35355(\beta + \beta \cot^2(\beta) - \cot(\beta))}{\left(\frac{\cot(\pi-\beta)}{\sqrt{2}} + \cot(\beta)\right)} \quad (23)$$

$$CCF_I = (G_2(\rho_0) * \sin(\beta) * C_2) / (\beta * C_1) \quad (24)$$



$$K_I = \sigma_{app} \sqrt{\pi a_j} CCF_I = K_{I_{max}} \quad (25)$$

6. MATERIAL USED AND SPECIMENS

The material used in this research is low carbon steel (EN 10219 S235JRH). It is a pipe with a circular section thickness about 1.5 mm and a diameter of about 75 mm. This research was done on several samples of this article. Some of these samples have a length of 100 cm, **Anil, 2015, Fig. 1** and other have a length of 50cm as in **Fig. 2**. The reason for this difference to test the effect of bending on the growth and behavior of the crack. This test was conducted under different environmental conditions to determine the effect of the moisture and heat factors on the growth of the crack.

7. MANUFACTURING OF DEVICE

This device was made of several parts of iron with different sections according to the required part. Also the technique of electric arc welding was used to connect these parts. The parts are cut using the cutting machine. After the cutting, the welding process is carried out to connect them together. However, most parts of this machine have the ability to switch when failure or damage occurs in one of these parts. This technique facilitated the work in many businesses on this machine for the fact that working on this device requires a change in the shape and position of the supports often to match the course of the research. A wooden plate was used to fix the parts of the machine. The dimensions of this plate are (122 cm x 244 cm) and thickness 1.5 cm. This plate has a hole in the middle to facilitate the passage of the hammer lever and to facilitate the examination of the pipe using the camera or naked eye. The dimensions of the parts of each other were developed using a laser device called (level) that allows the device to see the extent of the separation of these parts or deviation from each other, which adds the possibility of placing the parts with high accuracy. This device enables the possibility of conducting tests on pipes made of iron, carbon steel, aluminum, copper, and plastic. The design of this device includes the possibility of changing the height of the hammer to suit the amount of energy necessary and strong with the ability of the metal to withstand the shocks, Also it can work on the pipes of different length ranging from 50 cm to 150 cm and different diameters ranging from 2 to 4 inch. In addition, the researcher or worker on this device can control the environmental conditions to be operated from heat, humidity, and control where it can work in the areas of temperature ranging from 0°C to 100 °C. Also, control the humidity, where it can work in the humidity ratio ranging from 0% to 100%.

8. MATERIAL PROPERTIES

These properties are from **DIN EN 10219**

1. Chemical composition

Chemical composition is in percentage by mass as in **Table 1**.

2. Mechanical properties

These mechanical properties are measured at room temperature, as in **Table 2**

3. Physical properties

Physical properties for this material are shown in **Table 3**.



9. CRACK INITIATION

The crack was created manually by handsaw. This is because that the crack is difficult to accomplish using other machines. The length of the cut is about 24%, **Wilkowski, et al., 1994**, of the perimeter of the pipe. This percentage was based on previous research, where the ratio was a length of 56 mm and width of the crack is about 0.7 mm to 0.9 mm. This difference is due to the difference in the thickness of the cutting edge in the saw as well as the hand movement. Other percentages were chosen to indicate the possibility of conducting the search on different lengths of the crack. However, these lengths of (18mm, 25mm, 30mm, and 40mm) took a long time without any continuity in the growth of the crack.

10. RESULTS AND CALCULATIONS

Table 4 and **Table 5** show the calculations that must be used in this search, then it is used in the governing equations, **Table 6** and **Table 7**.

Results were obtained by using rig made for testing these specimens, as in **Fig. 3**, the tests were repeated again to ensure a close test result as well as to ensure the correct functioning of the rig. The results are shown in the **Fig. 7, Fig. 8, Fig. 9, and Fig. 10**

11. CONCLUSIONS

The purpose of this study is to determine the extent to which the crack is able to grow when shedding and how long it takes to grow these cracks. Some things need to be discussed to know what changes are made to these cracks and to make things better.

- 1- The number of cycles needed to grow the crack are reduced due to the effect of humidity because of the formation of oxides on the fracture surface.
- 2- The number of cycles needed to grow the crack in the specimens of length 50cm are increased because of the length due to the effect of bending stress in the pipes.

12. REFERENCES

- Anil, O., Erdem, R. T., Kantar, E., 2015, *Improving the Impact Behavior of Pipes Using Geofom Layer For Protection*, International Journal of Pressure vessel and piping, pages 52-64
- Al Laham S., Ainsworth R. A., 1999, *Stress Intensity Factor and Limit Load Handbook*, British Energy Generation Ltd., UK
- Bertram Broberg, K., 1999, *Cracks and Fracture* Academic press, pages 1-4, ISBN: 978-0-12-134130-5
- Forman, R. G., Kearney, V. E., Engle, R. M., 1967, *Numerical Analysis of Crack Propagation in Cyclic Loaded Structures*, pages 459-463
- G. M. Wilkowski, Gadiali, N., Rudland, D., Krishanswamy, P., Rahman, S., Scott, P., 1994, *Short Cracks in Piping and Pipe Welds*, Vol 4, no 1, page 78.



- Mcevely, A. J, 1996, *The Growth of Short Fatigue Crack*, Transaction of material science, Vol. 13, pages 1-5
- Stein, D., 2004, *Rehabilitation and Maintenance of Drains and Sewers*, technique technology center
- Wasiluk, B., Golos, K., 2000, *Prediction of Crack Growth Direction under Plane Stress For Mixed Mode I and II Loading*, pages 6

NOMENCLATURE

LEFM = linear elastic fracture mechanics
 MTS = multi-tasking staff
 da/dn = crack growth per cycle, m/cycle
 r,θ = polar coordinate, dimensionless
 σ_θ = circumferential stress near crack tip, Mpa
 k_1, k_2 = stress intensity factor, $Mpa\sqrt{m}$
 π = mathematical constant, dimensionless
 $\tau_{r\theta}$ = shear stress in cylindrical coordinate, Mpa
 $\sigma_x, \sigma_y, \tau_{xy}$ = component of stress tensor, Mpa
 ν = poison ratio, dimensionless
 E = young modulus, Gpa
 θ = angle of crack propagation, degree

Table 1. The chemical composition of the material.

Carbon	silicon	Manganese	phosphorus	sulfur	nitrogen
0.17	-	1.4	0.04	0.04	0.009

Table 2. Mechanical properties of the material.

Yield strength in N/mm^2 min for nominal wall thickness less than 16 mm	Tensile strength in N/mm^2 for nominal wall thickness less than 3 mm	Elongation % for nominal wall thickness less than 40 mm	Impact energy in J at a temperature of 20°C
235	360-510	24	27



Table 3. Physical properties of the material.

Density at 20°C in kg/dm ³	Modulus of elasticity kN/mm ² at 20°C	Thermal conductivity at 20°C in w/ m k	Spec. thermal capacity at 20°C J/kg k	Spec. electrical resistivity at 20°C Ω mm ² /m
7.85	210	54	461	0.15

Table 4. Calculations for 100cm specimens.

Outer diameter (OD)=0.075m inner diameter (ID)=0.0722m thickness (t)= 0.0014m Yield point= 235 Mpa modulus of elasticity (E)= 210Gpa high (h)=0.57m weight (w)= 6.7Kg effective length (l)= 1m			
Load applied	Moment of inertia	deflection	Bending stress
2279.3 N	$0.22 * 10^{-6} m^4$	0.0103 m	1949.1 Mpa

Table 5. Calculations for 50cm specimens.

Outer diameter (OD)=0.075m inner diameter (ID)=0.0722m thickness (t)= 0.0014m Yield point= 235 Mpa modulus of elasticity (E)= 210Gpa high (h)=0.57m weight (w)= 6.7Kg effective length (l)= 1m			
Load applied	Moment of inertia	deflection	Bending stress
2223.2 N	$0.22 * 10^{-6} m^4$	0.0018 m	1378.1 Mpa

Table 6. Calculations using cyclic load equations for 100cm specimens.

Type of test	k1		k2		Slop (m)	
	LHS	RHS	LHS	RHS	LHS	RHS
without	$1.33*10^9$	$1.33*10^9$	$1.35*10^9$	$1.35*10^9$	6.91	8.4
Humidity 1 hour	$1.3*10^9$	$1.33*10^9$	$1.31*10^9$	$1.36*10^9$	6.04	4.4
Humidity 2 hour	$1.31*10^9$	$1.32*10^9$	$1.36*10^9$	$1.37*10^9$	6.2	3.4



Table 7. Calculations using cyclic load equations for 50cm specimens.

Type of test	k1		k2		Slop (m)	
	LHS	RHS	LHS	RHS	LHS	RHS
without	1.33×10^8	1.33×10^8	1.35×10^8	1.35×10^8	2.05	7.6
Humidity 1 hour	1.3×10^8	1.33×10^8	1.31×10^8	1.36×10^8	1.85	2.7
Humidity 2 hour	1.31×10^8	1.32×10^8	1.36×10^8	1.37×10^8	2.19	2.4

Note: the data in table 4, table 5, table 6 and table 7 is obtained using MATLAB program by Applying equations in **point 5**



Figure 1. Two samples of length 100cm.



Figure 2. Two samples of length 50cm.

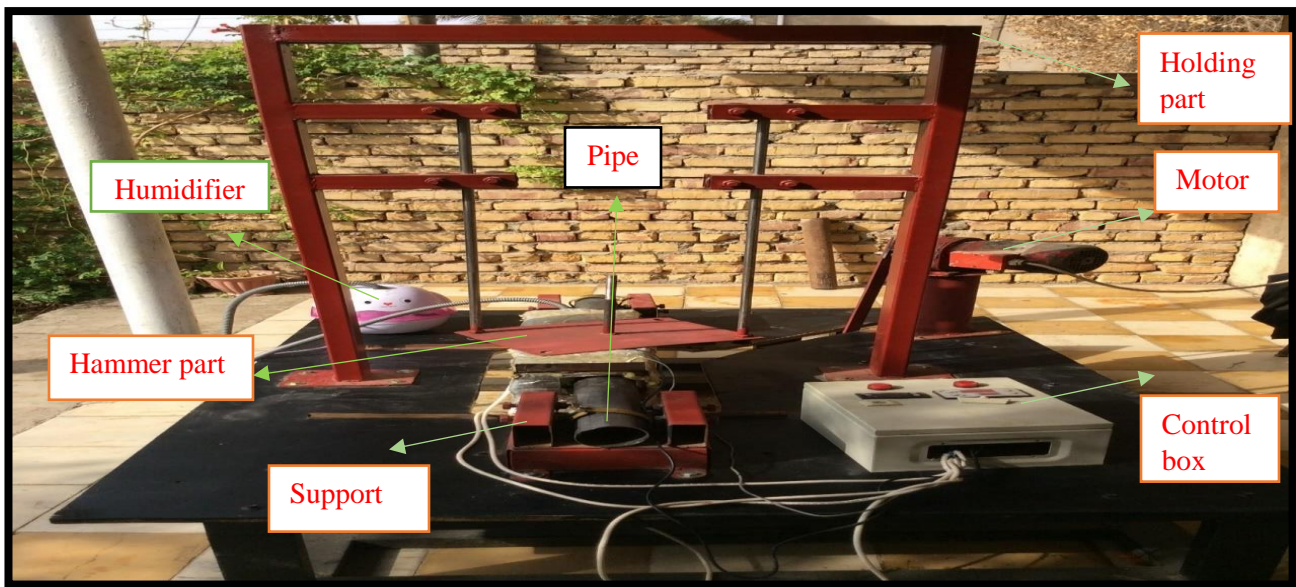


Figure 3. The device used to test the specimens.

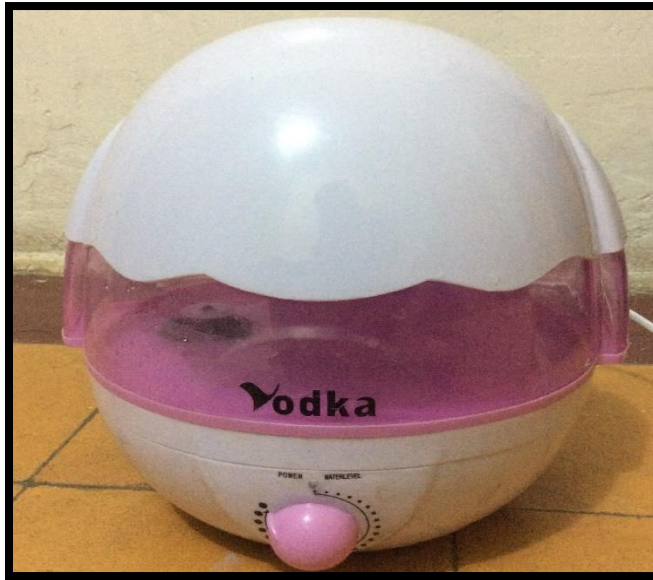


Figure 4. Humidifier device.

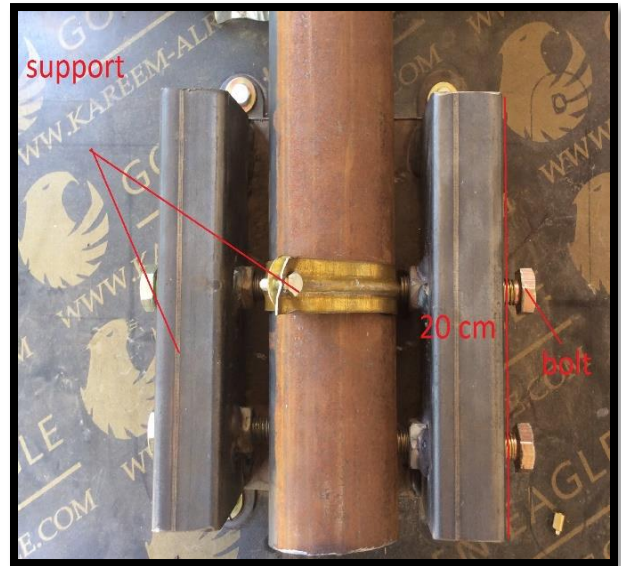


Figure 5. Support.



Figure 6. Close up photo showing the crack and crack growth.

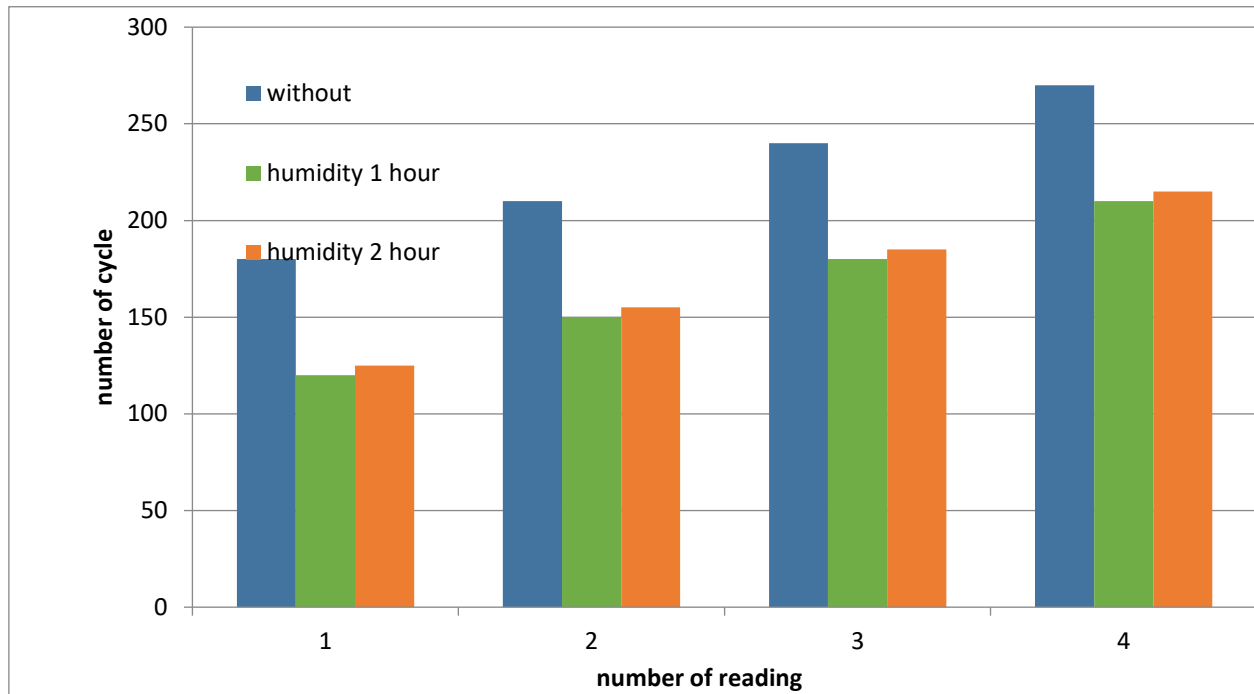


Figure 7. The number of cycles of every specimen of length 100cm.

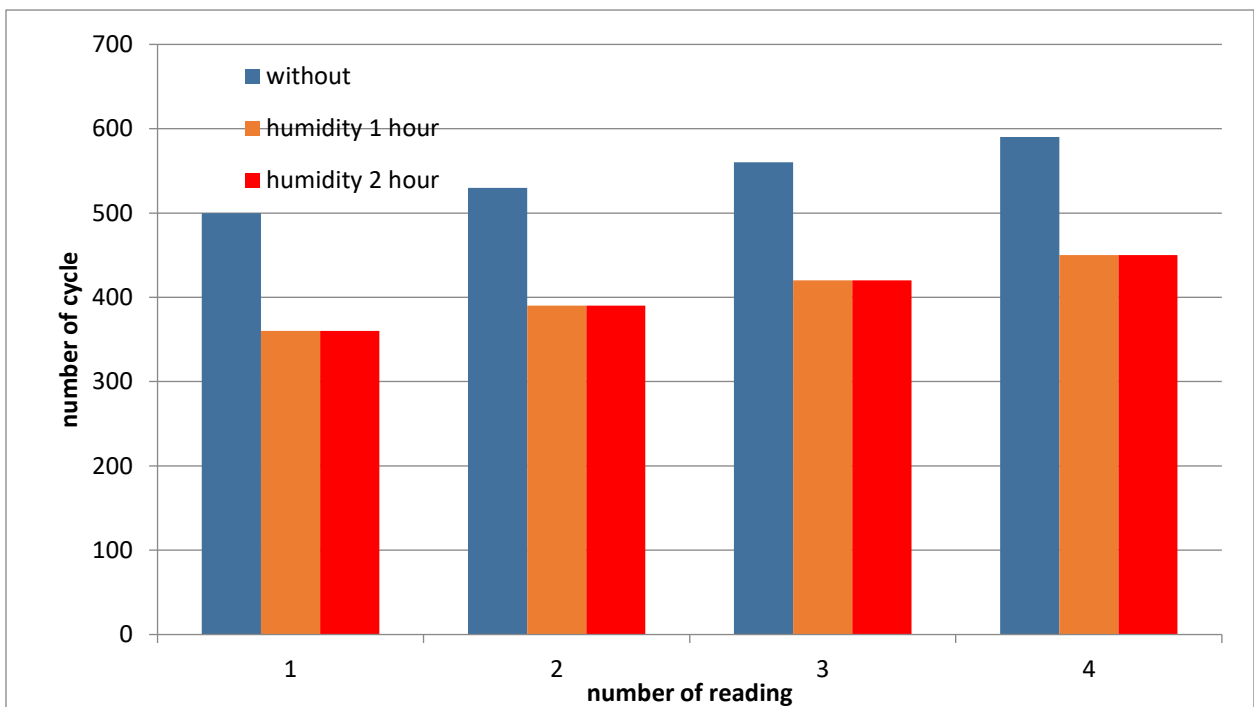


Figure 8. The number of cycles of every specimen of length 50cm.

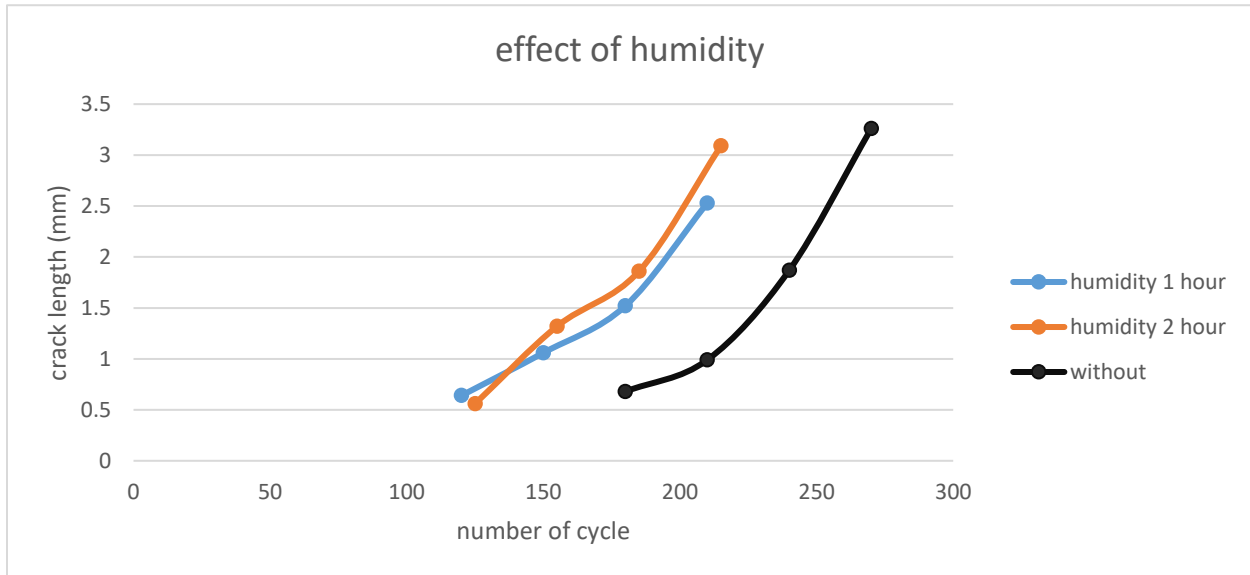


Figure 9. The effect of humidity on the crack growth in the right side (100cm).

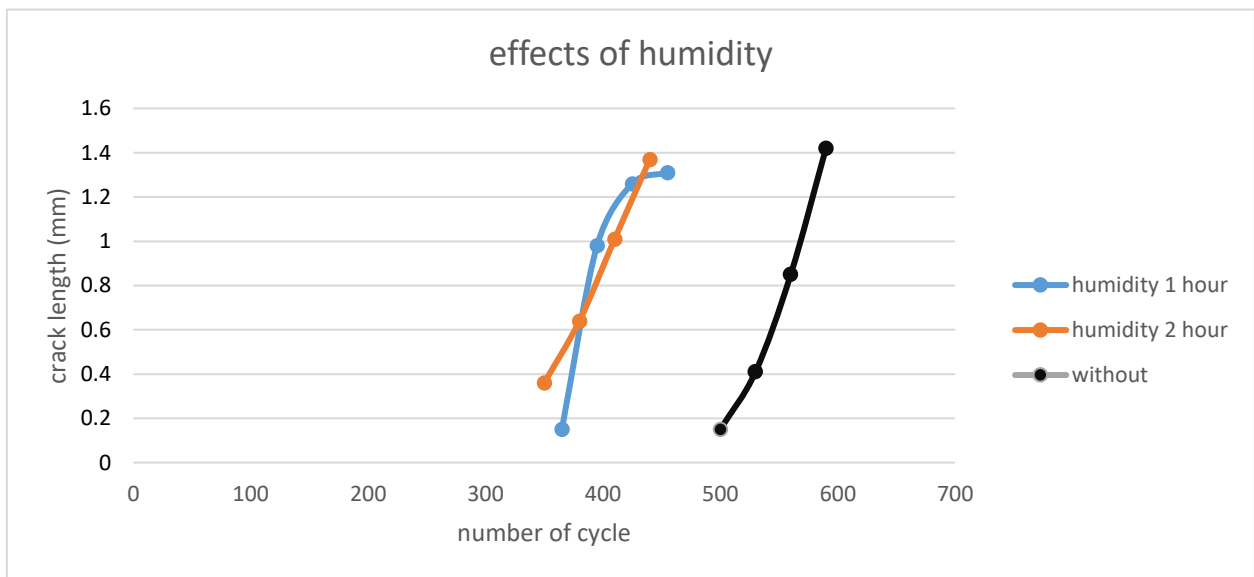


Figure 10. The effect of humidity on the crack growth in the right side (50cm).